Simulation of Surface EMG Signals for a Multi-layer Volume Conductor with Triangular Model of the Muscle Tissue

(Article begins on next page)

Simulation of Surface EMG Signals for a Multi-layer Volume Conductor with Triangular Model of the Muscle Tissue

Luca Mesin

Abstract—**This study analytically describes surface electromyogram (sEMG) signals generated by a model of a triangular muscle, i.e., a muscle with fibres arranged in a fan shape. Examples of triangular muscles in the human body are the deltoid, the pectoralis major, the trapezius, the adductor pollicis. A model of triangular muscle is proposed. It is a sector of a cylindrical volume conductor (with the fibres directed along the radial coordinate) bounded at the muscle/fat interface. The muscle conductivity tensor reflects the fan anisotropy. Edge effects have been neglected. A solution of the non space invariant problem for a triangular muscle is provided in the Fourier domain. An approximate analytical solution for a two plane layer volume conductor model is obtained by introducing a homogeneous layer (modelling the fat) over the triangular muscle. The results are implemented in a complete sEMG generation model (including the finite length of the fibres), simulating single fibre action potentials. The model is not space invariant due to the changes of the volume conductor along the direction of action potential propagation. Thus the detected potentials at the skin surface change shape as they propagate. This determines problems in the extraction and interpretation of parameters. As a representative example of application of the simulation model, the influence of the inhomogeneity of the volume conductor in CV estimation is addressed (for two channels; maximum likelihood and reference point methods). Different fibre depths, electrode placements and small misalignments of the detection system with respect to the fibre have been simulated. The error in CV estimation is large when the depth of the fibre increases, when the detection system is not aligned with the fibre and close to the innervation point and to the tendons.**

Index Terms— electromyography, EMG modelling, volume conductor, spatial frequency, triangular muscles

I. INTRODUCTION

THE simulation of surface electromyogram (sEMG) signals is important for a deeper understanding of the physiological mechanisms of muscle contraction [20]. Simulations are useful for the estimation of physiological variables (inverse problem) [37]. Furthermore, they can help in the choice of the detection system [5][7][13] in the interpretation of experimental results [6][32], in designing and testing algorithms for information extraction [8], and for didactic purposes [1][23][24][36].

Different types of volume conductors have been studied, both by analytical and numerical methods [15][21][28][34]. Analytical solutions can be obtained only in specific cases, while numerical methods apply also in more complex situations [21]. Nevertheless, analytical solutions are valuable: to check the accuracy of numerical methods, to reduce the computational time, to determine the theoretical dependence of the solution on specific parameters of the system. Thus, it is important to focus on numerical methods only when the geometry of the volume conductor and the properties of its conductivity tensor are too complex, and such methods are justified by the application at hand.

Focusing on analytical methods, generation models of sEMG are available for the following types of volume conductors: isotropic, homogeneous, infinite medium [4][23][24]; multi layer models for planar [10] and cylindrical [2][14][17] volume conductors; volume conductors with local [26] and with distributed [27] inhomogeneity; bipinnate muscle [25]; muscle with fibres inclined with respect to the detection surface [25].

Most models proposed in the literature assume the volume conductor to be space invariant in the direction of propagation of the intracellular action potentials. In such a case, for infinite length fibres, the potential distribution over the skin can be described as a propagating wave, for which the spatial coordinate along the fibre direction and the time coordinate are related by the constant velocity of propagation (conduction velocity, CV) [12]. For space invariant models a detection channel (sum of the potentials detected at different points) can

be considered as a spatial filter [3][7]. When considering finite length fibres, the source changes shape with time due to the generation and extinction of the action potentials at the end-plates and tendons. The generation and extinction affect the recorded surface potential with the onset of non propagating

components, which constitute an important problem in the estimation of muscle fibre CV [3][11][12], and in spatial filter selectivity [1][7][13].

In addition to finite length fibres, the volume conductor may also introduce shape variations in the detected surface potentials due to inhomogeneities (veins, glands, skin or fat thickness changes) [26][27][34], or to an arbitrary path of the muscle fibres [15], which can also change in time with muscle shortening, as occurring in dynamic contractions [27]. Generation models can help in understanding the effects of a single characteristic of the volume conductor on the detected signals.

Human muscles can be schematically classified in four general types (see Figure 1a), which are the parallel or fusiform (e.g., brachial biceps, sartorius, rectus abdominis), the circular (e.g., external anal sphincter), the pinnate muscle (unipinnate, e.g. soleus; bipinnate or multipinnate, e.g., rectus femuris, subscapularis), the triangular (e.g., deltoid, pectoralis major, trapezius, adductor pollicis). Parallel muscles have fibres arranged parallel to the line of action (muscle pull) and are specialised for movements requiring great excursion and/or velocity. Circular muscles have circular fibres and are specialised in closing sphincters. In pinnate muscles, fibres lie at an angle to the line of action; they are specialised for force production (as the pinnation increases the cross-sectional area for the same volume of the muscle). In triangular muscles, the fibres are radially arranged. They are specialised for altering the line of action, given the arrangement of the motor units in different directions. For parallel and circular muscles, the model is space invariant (if no inhomogeneities are introduced in the other layers constituting the volume conductor). Also pinnate muscles can be modelled (at a first approximation) by a space invariant model, by simply considering a model of a parallel muscle, rotating the fibres and placing the tendons at an angle with respect to the fibres. On the contrary, a bipinnate muscle (in which oblique fibres converge to both sides of a central tendon) is not space invariant, as the muscle conductivity properties change completely from one side to the other side of the pinnation line (which means that it is not homogeneous). A triangular volume conductor is not space invariant. Indeed, the conductivity properties are different in the region where fibres approach each other and where they are more separated.

Parallel, circular and pinnate muscles were addressed in the literature [10][14][25], but no modelling work aimed at analytically describing sEMG signals generated by a triangular muscle has been reported. This study addresses this issue, providing the solution of the inhomogenous, anisotropic problem, with an implementation of the results in a complete sEMG generation model (including finite length fibres), and shows representative results of the application of the model proposed.

II.   METHODS

The bioelectrical problem of sEMG simulation can be considered as quasi-static [18]. Assuming insulation at the surface, the following Poisson problem can be written:

$$\begin{cases} -\nabla \cdot (\underline{\underline{\sigma}} \nabla \varphi) = I & \Omega \\ \underline{\underline{\sigma}} \nabla \varphi \cdot n = 0 & \partial\Omega \end{cases} \quad (1)$$

where φ is the potential (V), I the current density source (A/m^3), $\underline{\underline{\sigma}}$ the conductivity tensor (S/m), Ω and $\partial\Omega$ the volume conductor domain and its boundary, respectively, n the normal vector to $\partial\Omega$.

In the following section the Poisson problem (1) is written in the case of the triangular muscle under consideration.

2.1 Model of a Triangular Muscle

The considered mathematical model of the volume conductor is represented in Figure 1b, 1c. It is a plane layer model, with a homogeneous isotropic layer (modelling fat, or skin; in the following I'll refer to such a layer as the fat layer) and an inhomogeneous, anisotropic layer (the muscle layer). The simulated muscle conductivities are 0.5 S/m in the direction of the fibres and 0.1 S/m in the transversal directions; the fat is isotropic, with a conductivity of 0.02 S/m (as in [14]).

The fat layer is a homogeneous layer in $0 < z < d$. Laplace equation should be solved in the fat layer (as the conductivity tensor is isotropic and homogeneous and no electrical sources are present in the fat layer). The fat layer is insulated at $z = d$.
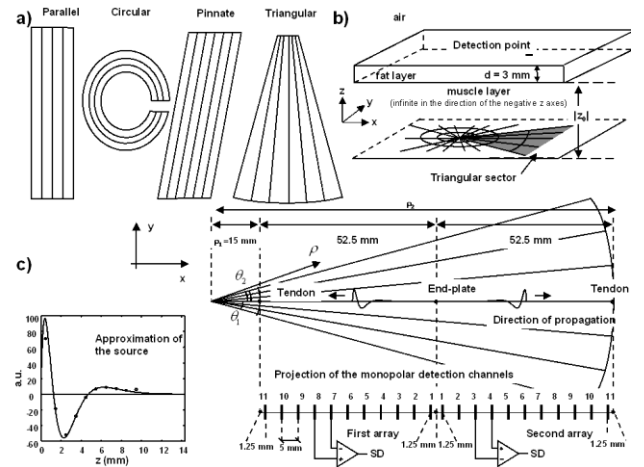
Figure 1: Schematic representation of the mathematical model. a) Classification of the human muscles into four types, depending on the fibres arrangement. b) Three dimensional representation of the volume conductor under consideration. The muscle conductivities are 0.5 S/m in the direction of the fibres and 0.1 S/m in the transversal directions; the fat layer is isotropic, with a conductivity of 0.02 S/m. c) Two dimensional view of a triangular muscle, propagating bioelectric sources (with the description of their sampling) and relative position of the detection arrays.

The muscle layer is semi-infinite (infinite in the x, y directions; defined only in z<0). The conductivity tensor is diagonal in a cylindrical coordinate system. The triangular muscle is modelled as a sector of the space (bounded at the muscle/fat interface). The fibres are arranged in a fan shape, i.e. in the direction of the radial variable of the cylindrical coordinate

system. A higher (longitudinal) conductivity is considered along the fibres, and a lower (transversal) conductivity is imposed in the orthogonal directions. Thus, the following Poisson equation is considered

$$\frac{\sigma_L}{\rho}\frac{\partial}{\partial\rho}\left(\rho\frac{\partial\varphi}{\partial\rho}\right)+\frac{\sigma_T}{\rho^2}\frac{\partial^2\varphi}{\partial\theta^2}+\sigma_T\frac{\partial^2\varphi}{\partial z^2}=-\frac{1}{\rho}\delta(\rho-R)\delta(\theta)\delta(z) \quad (2)$$

where ρ,θ,z are the independent variables in the cylindrical coordinate system, δ is the Dirac delta function, σ_L is the longitudinal conductivity, σ_T the transversal one, and the source is located at the point $\vec{r}_s=(\rho=R,\theta=0,z=0)$, where R is an arbitrary non negative real number. Eq. (2) models a cylindrical muscle which can be considered as a triangular muscle under the hypothesis of neglecting edge effects, given by the conditions to be imposed at the angular and radial extremes of the muscle (indicated by $\theta=\theta_1$, $\theta=\theta_2$ and $\rho=R_1$, $\rho=R_2$ in Figure 1c). The local conductivity along the radial coordinate is the same in each point except $\rho=0$, where the conductivity is σ_L in all directions (there are fibres exiting in all directions from $\rho=0$). Considering general different points of the muscle layer, the conductivity properties change, as in general the direction of maximal conductivity is different at different points. This means that the muscle layer is inhomogeneous. It is worth noticing that also the model of a sphincter proposed in [14] is inhomogeneous, for the same reason, but it is space invariant in the direction of propagation.

Interface conditions between the muscle and the fat layers are the continuity of the potential and of the current density perpendicular to the boundary surface. The potential vanishes at infinity.

2.2 Simulation of single fibre action potentials

The impulse response in cylindrical coordinates was fully described in [14], where models of a limb (with fibres along the z axis) and of a sphincter (with fibres arranged in the angular direction) were discussed. For the problem at hand, the fibres are arranged along the radial direction. The impulse response is given by the following expression (refer to [14] for the details)

$$\varphi(x,\theta,z)=\sum_{k_\theta=-\infty}^{+\infty}\int_{-\infty}^{+\infty}\Gamma(x;k_z,k_\theta)e^{jk_zz}\mathrm{d}k_z e^{jk_\theta\theta} \quad (3)$$

where $x=k_z\sqrt{\frac{\sigma_T}{\sigma_L}}\rho$, k_θ and k_z are the spatial frequencies, and

$$\Gamma(x;k_z,k_\theta)=\begin{cases}\frac{1}{\sigma_\rho}I_n\left(k_z\sqrt{\frac{\sigma_T}{\sigma_L}}R\right)K_n(x) & \text{for} \quad \rho>R \\ \frac{1}{\sigma_\rho}K_n\left(k_z\sqrt{\frac{\sigma_T}{\sigma_L}}R\right)I_n(x) & \text{for} \quad \rho<R\end{cases} \quad (4)$$

where $n=k_\theta\sqrt{\frac{\sigma_T}{\sigma_L}}\rho$, $I_n(x)$, $K_n(x)$ are modified Bessel functions of order n of the first and second type, respectively. The volume conductor considered is not space invariant. This is the main difference between such a model and the model of

limb and sphincter muscles already considered in [14]. For a space invariant volume conductor impulse responses associated to impulses placed at different points along a fibre are the same except for a translation. For non space invariant volume conductors, impulse responses change shape by moving the impulse along a fibre. This means that for such volume conductors (and in particular for the triangular muscle studied here) it is necessary to sample the fibre path and to simulate the impulse response at each sampling point.

The radial coordinate was sampled with 1 mm step. This allows to have a sampling (4 kHz) preserving information for a signal propagating at 4 m/s (as sEMG signals have a band of 10-400 Hz).

A recent work explains how to obtain an approximate analytical solution for a multi-layer model once the solution for an infinite layer is known [29]. The solution in the muscle is a linear convolutive mixture of the potential and of its normal derivative for an infinite triangular muscle at z=0. The resulting solution is not exact, as the volume conductor is not space invariant. The goodness of the approximation is given by the localisation of the kernels, which are indeed concentrated around the position of the impulse source.

The potential is given by Eq. (3). The normal derivative can be obtained by inverting the Fourier transform of the solution after multiplication by jk_z. To apply directly the method proposed in [29], the potential and its normal derivative must be expressed in Cartesian coordinates: the cylindrical coordinates were transformed into Cartesian ones by a triangle-based linear interpolation.

The transmembrane current (which is the bioelectrical source of the problem) is modelled as the second spatial derivative of the transmembrane potential, mathematically described in [33]. A support 10 mm long was considered for the source. It was sampled by 10 impulses, spaced by 1 mm step (in Figure 1c the amplitude of each of the considered impulse is indicated by a dot). The first *9* impulses had amplitude proportional to the integral of the source in the correspondent sampling interval. The last impulse equals the sum of the previous 9, with a minus sign. This value corresponds to the integral from the 9th sampling point to infinity and allows to conserve charges (Figure 1c).

The surface potential can be obtained by studying the source generation, travelling and extinction. The generation was simulated by moving the source out from the innervation point (two impulses each step, one on the left, the other on the right of the innervation point) and putting an impulse at the innervation point to conserve charges. The reverse process of the generation of one source was used for simulating its extinction.

The detection of a single fibre action potential from a point electrode was obtained by evaluating the potential in the detection point for each simulated step. The estimation of the potential at a generic detection point (not corresponding to a sampling point) is obtained in the Fourier domain, in order to preserve resolution.
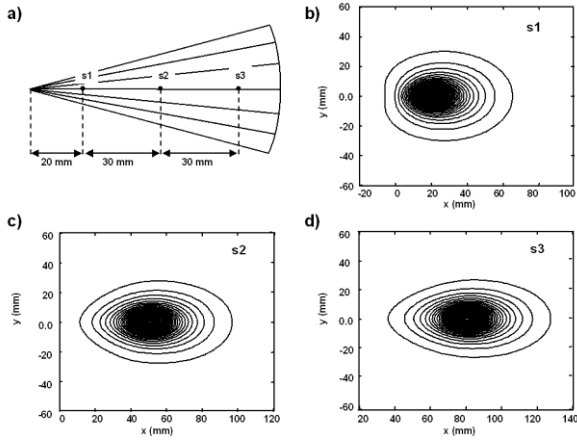
Figure 2: Examples of impulse responses (volume conductors as described in Figure 1b, 1c, with $|z_0| = 4mm$). Positions of three impulse sources, a), and corresponding potentials, b), c), d) (50 level curves are shown; the levels are a uniform sampling from the maximum point to zero, maximum value and zero excluded). The non space invariance of the volume conductor determines shape changes in the impulse responses related to translated impulses.

2.3 Signal processing
The effect of the simulated non space invariant volume conductor on CV estimation was addressed. CV was estimated as the ratio of the distance between the centres of two detection channels (single or double differential) and the delay of propagation of the potentials. Two approaches for estimating the delay were used. The first is maximum likelihood method [9]. As two channels have been considered for each estimate, the method is equivalent to the spectral matching estimator [22], or to the cross-correlation function method [30][31], often used in the applications. The second approach considered is based on the detection of reference points [19]. The maximum and the minimum peak (estimated using a second-order polynomial interpolation of the samples [19]) were considered as reference points.

III.   RESULTS

The model described was used to generate single fibre action potentials. The geometry of the volume conductor is shown in Figure 1b and 1c. Two arrays of 11 monopolar electrodes were simulated, as shown in Figure 1c. The centres of the two arrays (i.e., the electrodes number 6) are in the mean points between the innervation zone and one tendon (each tendon corresponding to one of the two arrays) of the fibres which are under the detection arrays.
3.1 Effect of the non space invariant volume conductor
The effect of inhomogeneity is studied in Figure 2, where impulse responses at different points are shown. As a consequence of the inhomogeneity of the conductivity tensor, the impulse response changes shape when the impulse is located at different points. As the fibres become parallel at infinity, we can expect that the impulse response approaches

that of a parallel muscle as the distance from the centre of the polar coordinate system $\rho = 0$ increases. From Figure 2, we can note that the impulse response becomes more and more symmetric (with respect to the maximum point) as the distance of the location of the impulse from $\rho = 0$ increases.

Figure 3 depicts a quantitative comparison between simulated surface potentials associated to a model of parallel muscle fibres and the proposed model of triangular volume conductor. The response of the volume conductors to the source (constituted by the 10 points indicated in Figure 1c) is considered. Figure 3a, 3b, 3c show examples of surface potentials from models of a parallel muscle (Figure 3a) and of a triangular muscle with source located at 25 mm (Figure 3b) and 75 mm (Figure 3c) from the axis $\rho = 0$. The surface potentials have been translated in space in order to be comparable. The potential relative to the triangular volume conductor changes shape by translating the source. Furthermore, such a potential is qualitatively more different than that corresponding to the model of the parallel muscle as the source approaches the axis $\rho = 0$. To quantify the effect of the volume conductor on the simulated potential, the mean square error between the potentials associated to the triangular and to the planar volume conductors was calculated (after alignment), for different positions of the source (transmembrane potential approximated as in Figure 1c) along the radial direction and for three depths of the fibres within the muscle. In Figure 3d such a square error is reported as a percentage with respect to the mean energy of the two considered potentials. The percentage square error is more than 10% near $\rho = 0$ and decreases monotonically with increasing distance from $\rho = 0$. It is worth noticing that such a percentage error gives a global information: the distortion in shape of signals detected from a channel depends on the actual location of the detection point.
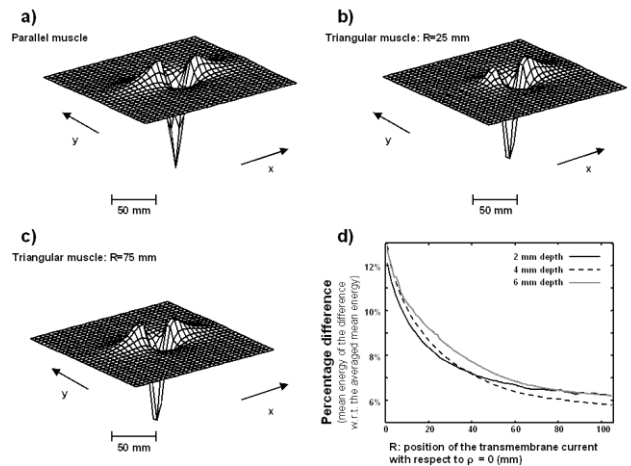

Figure 3: Quantitative comparison between simulated surface potentials associated to a model of parallel muscle and the model of triangular volume conductor. The response of the volume conductors to the source (described in Figure 1c) is

considered. Examples of surface potentials from models of a parallel muscle, a), and of a triangular muscle with source located at *25 mm*, b), and *75 mm*, c), from the axis $\rho = 0$ (the distances are computed from the axis $\rho = 0$ to the impulse of the source closest to the axis $\rho = 0$). Depth of the simulated fibre within the muscle is *4 mm*. The surface potentials have been translated in space in order to be comparable. The mean square error between the potentials associated to the triangular and the planar volume conductors (i.e., the mean energy of the difference between the two potentials) for different positions of the sources along the radial direction and for three depths of the fibres within the muscle is shown in d), as a percentage with respect to the mean energy of the two considered potentials.

3.2 Effect of the fibre location on the single fibre surface potentials
To study the effect of the proposed volume conductor on the signals detected from electrode arrays, the two arrays in Figure 1c were considered. Comparing the signals detected from the two arrays, it is possible to quantify the effect of the geometrical arrangement of the fibres and of the inhomogeneous conductivity tensor. In Figure 4, simulated monopolar (Figure 4a) and single differential (Figure 4b) signals are shown, for 3 depths within the muscle and 3 angles of the fibres with respect to the detection arrays, with simulated CV of the action potential along the fibre equal to 4 m/s. The distribution of the fibres determines a transversal distance between a fibre and the detection points (with the exception of the fibres which are under the arrays) that changes as a function of the detection point. This affects the signals related to fibres directed with a finite angle with respect to the detection arrays. In Figure 4 the signals related to fibres with $\theta = 5°$ and $\theta = 10°$ change amplitude between channels and between the two arrays. Considering the fibres located under the detection arrays (which means $\theta = 0°$), the geometry of the muscle and of the detection system is symmetric with respect to the innervation zone. If the conductivity tensor was homogeneous, as in the case of a parallel muscle, the signals detected from the two arrays would be exactly the same. The simulated signals in such a case give indication of the effect of the inhomogeneity of the conductivity tensor. The simulated signals shown in Figure 4 indicate that the amplitude of the signals associated to fibres with $\theta = 0°$ does not change, as expected. There are small shape variations of the potentials across channels.

3.3 CV estimation
The effect of the inhomogeneous volume conductor on CV estimation was addressed. The same simulated positions of the fibre within the muscle as described in Section 3.2 were considered. The value of the simulated CV was 4 m/s. The results of CV estimations obtained from each pair of the simulated single and double differential channels are shown in Figure 5 (were the simulated CV, 4 m/s, is also shown), in the

case of the maximum likelihood method. The estimates obtained from the first and the second array can be compared. There are small differences between CV estimates obtained with the signals from the two arrays, considering the results from the fibres with $\theta = 0°$. These differences are only due to the inhomogeneity of the conductivity tensor. The differences in CV estimates associated to fibres with $\theta > 0°$ are due both to the inhomogeneous conductivity tensor and to the path of the fibres (which can be referred to as the effect of geometry).

The estimates from the second array are affected by a greater error with respect to those from the first one, as the fibres are more distant from the second detection array than from the first. In such a case, generation and extinction contribute more strongly to the detected signals, giving larger error in CV estimation. These general considerations hold for both the CV estimates obtained from the single and the double differential signals. The double differential detection is more selective than the single differential one [13]. Thus, it is expected that the double differential filter can reduce the effect of non propagating components and improve CV estimates. Indeed, for the first array and superficial fibres, we can note that CV estimates from double differential signals are closer to the simulated CV with respect to those from single differential signals. However, the double differentiation enhances the shape differences between signals detected by two channels. These differences are essentially due to the geometry of arrangement of the fibres and to the inhomogeneity of the conductivity tensor, and determine an error (which could be both positive or negative) in the CV estimates.
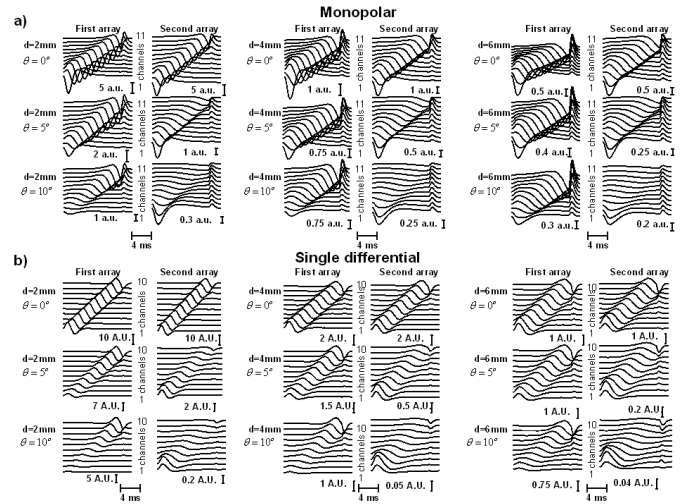
Figure 4: Simulated single fibre action potentials. Monopolar, a), and single differential, b), detection, for 3 depths within the muscle and 3 angles of the fibres with respect to the detection arrays (shown in Figure 1c). Simulated muscle fibre CV is 4 m/s. The signals related to fibres with $\theta = 5°$ and $\theta = 10°$ change amplitude between channels and between the two arrays. Considering the fibres located exactly under the detection arrays (which means $\theta = 0°$), the geometry of the

muscle and of the detection system is symmetric with respect to the innervation zone, but the simulated signals are not symmetric, giving indication of the effect of the inhomogeneity of the conductivity tensor.

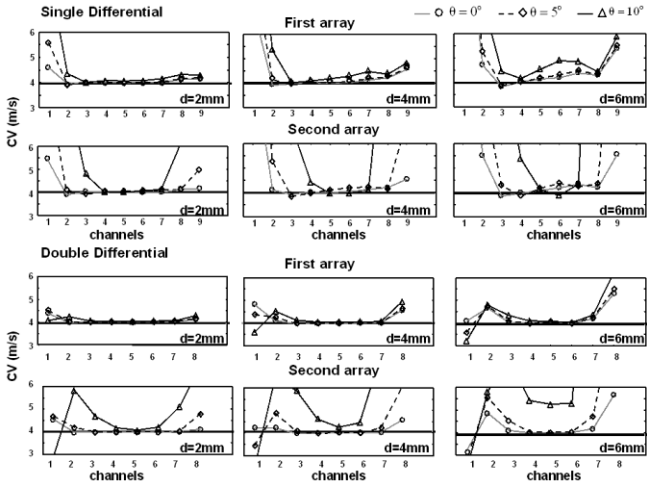**Figure 5**: Effect of the inhomogeneous triangular volume conductor on CV estimation. Simulated CV equal to 4 m/s. CV estimation (maximum likelihood method, [9]) was performed on each pair of the simulated channels (simulated arrays shown in Figure 1c), for single and double differential detection, for 3 depths of the fibres within the muscle and 3 angles of the fibres with respect to the detection arrays (same signals shown in Figure 4). It is possible to compare the estimates obtained from the first and the second array. Comparing the results from the fibres with $\theta = 0°$, it is possible to note small differences (mainly for channel pairs close to the innervation zone and tendons) between the corresponding channels of the two arrays. Such differences are due to the inhomogeneity of the conductivity tensor. The differences in the CV estimates for the two arrays and associated to fibres with $\theta > 0$ are due both to the inhomogeneous conductivity tensor and to the positions of the fibres with respect to the array.

In order to better discriminate between the effect of the geometry and that of the conductivity tensor, the same simulations were repeated by substituting the inhomogeneous muscle conductivity tensor with a homogeneous one (anisotropic muscle with direction of maximum conductivity along the x axis, same longitudinal and transversal conductivity as for the inhomogeneous conductivity tensor). As an indication of the variation in CV estimates obtained from the signals simulated by the two models, the mean of the absolute value of CV difference was chosen, fixing the depth of the simulated fibre in the muscle and the spatial filter (i.e., computing the mean over the channel and the angle). The considered CV values were restricted to those within the range 2-8 m/s. The results are reported in Table 1. The differences are higher when the active fibre is deeper and when the array is closer to the point of fibre convergence (i.e., the axis $\rho = 0$, in line with Figure 3). Even if the perturbation effect of the

volume conductor is not very high (about 10%, see Figure 3), the differences in CV estimations are important (not shown results indicate that the largest differences are obtained when the detection system is not aligned with the active fibres). This indicates the importance of a detailed description of the anatomy when the validation of algorithms for parameters extraction is addressed.

Table 1: Comparison between the proposed inhomogeneous model and a model with homogeneous conductivity tensor in the muscle layer (CV values restricted to the range 2-8 m/s).

Mean of the absolute value (computed over the channels and the angles) of the difference in CV estimates (m/s) obtained from two models of the conductivity tensor				
	First array		**Second array**	
Depth within the muscle	**Single differential detection**	**Double differential detection**	**Single differential detection**	**Double differential detection**
2 mm	0.29	0.67	0.08	0.04
4 mm	0.41	0.98	0.16	0.09
6 mm	0.61	1.20	0.30	0.13

Table 2: Comparison of maximum likelihood and reference points approach for CV estimation (mean and standard deviation computed over the channels and the angles are reported; CV values restricted to the range 2-8 m/s).

CV estimates (mean and standard deviation, m/s) – first array					
Depth within the muscle	**Single differential detection**			**Double differential detection**		
	Max likelihood	**Max peak**	**Min peak**	**Max likelihood**	**Max peak**	**Min peak**
2 mm	4.2 (0.5)	4.4 (1.0)	3.9 (0.3)	4.3 (0.8)	4.0 (0.7)	4.0 (0.2)
4 mm	4.4 (0.8)	4.3 (0.8)	4.1 (0.7)	4.5 (1.0)	3.8 (1.0)	4.1 (0.4)
6 mm	4.4 (0.5)	4.4 (1.0)	3.9 (0.5)	4.5 (1.1)	3.8 (0.8)	4.2 (0.5)
CV estimates (mean and standard deviation, m/s) – second array					
Depth within the muscle	**Single differential detection**			**Double differential detection**		
	Max likelihood	**Max peak**	**Min peak**	**Max likelihood**	**Max peak**	**Min peak**
2 mm	4.2 (0.3)	4.1 (0.7)	4.2 (0.3)	4.1 (0.1)	4.3 (0.4)	4.0 (0.1)
4 mm	4.4 (0.7)	4.0 (0.8)	4.5 (0.7)	4.2 (0.3)	4.1 (0.1)	4.0 (0.2)
6 mm	4.6 (0.8)	4.0 (0.6)	4.3 (0.8)	4.3 (0.6)	4.2 (0.3)	3.9 (0.3)

The maximum likelihood method was finally compared with two methods based on reference points. Means and standard deviations of CV estimates are shown in Table 2. CV values were restricted to those within the range 2-8 m/s. The methods based on reference points are less affected by shape changes of sEMG signals at different channels (giving a lower information on the effect of the volume conductor inhomogeneity: for this reason the maximum likelihood method was considered in Figure 5).

IV.   DISCUSSION AND CONCLUSIONS

In this paper the problem of analytically describing the sEMG signal generation from a volume conductor (a model of a triangular muscle) which is not space invariant along the direction of propagation of the sources is investigated.

The model is a simplification of the real conditions because 1) a planar, semi-infinite, two layer (but the extension to more than two layers is straightforward [29]) volume conductor with rectilinear fibres was considered, 2) edge effects due to the presence of other tissues surrounding the muscle are neglected.

However, the anatomical condition is quite complex compared to previous works. Indeed, there is only one other work in the literature which analytically addressed the issue of describing the sEMG signal generation from muscle tissues with different fibre directions, i.e., a bipinnate muscle [25]. The effect of the geometry and of the conductivity tensor of a bipinnate muscle on simulated sEMG signals was also addressed numerically in [15]. As in the case of a bipinnate muscle, the non space invariance of the triangular muscle determines shape variations of the single fibre action potentials detected at different points along the fibre direction. The effect of the non space invariance on the surface potential can be addressed by comparing the potential related to a non space invariant model to that obtained by a space invariant one. The mean square error of the simulated signal on all the detection surface with respect to that relative to a space invariant plane layer model is a function of the position of the bioelectric source, with larger values closer to the point of convergence of the fibres.

The proposed model, together with those developed in [10][14][25], allows to describe analytically the four main types of muscle fibre arrangements, i.e., the parallel [10], the pinnate ([10] for unipinnate, [25] for bipinnate), the circular [14] and the triangular (this paper).

The approach proposed for the solution of the problem is derived from previous works [10][14][29]. The solution was investigated in the bi-dimensional Fourier domain, as previously done; the solution in cylindrical coordinates was used, with a slight adaptation to the case at hand; the method proposed in [29] for the solution of Poisson problems in multi-layer volume conductors was used. The approach implies issues to be carefully addressed in the numerical implementation of the solution. In the case of space invariant systems, as those analysed in [10], the solution is only shifted in space if the source is shifted. For systems which are not space invariant, the impulse response must be computed at each location of the source. Some scaling properties of the impulse response have been exploited (see Appendix). They could help in designing efficient numerical methods for the evaluation of the impulse response of the Poisson problem for the considered volume conductor with different depths of the impulse.

The availability of the model may help in interpreting signals generated by muscles with more complex architectures than those comprised of fibres all parallel with respect to each other. In particular, the fact that the potentials detected over the skin along the fibre direction may change in shape is important for practical reasons, such as the estimation of muscle fibre CV. The problem of estimating CV from simulated signals from non space invariant volume conductors (studied by analytical methods) has been recently addressed in [16] for the case of a volume conductor presenting a local, spherical inhomogeneity (modelling a gland, a blood vessel or another local inhomogeneity), and in [27] for the case of smooth conductivity variations in the fat layer (modelling a concentration of glands or small vessels, scars or other structures). Some results concerning CV estimation are also shown here, using both maximum likelihood and reference point approach. Both single and double differential signals were simulated. More attention was given to CV estimates from maximum likelihood method, as they reflect the global effect of the inhomogeneous volume conductor on the simulated signals. In both cases of single differential and double differential detection, the estimates are strongly affected by the geometrical arrangement of the fibres and slightly affected by the inhomogeneous conductivity tensor. Nevertheless, CV estimates from signals simulated by using a homogeneous model of the muscle conductivity tensor differ substantially from those obtained using the proposed simulation model (mainly when the detection system is not aligned with the active fibre). This indicates the importance of a precise description of the anatomy. The error in CV estimates is large when the depth of the fibre increases, when the detection system is not aligned with the fibre and close to the innervation point and to the tendons. Errors in CV estimation was lower than 10% only in the case of superficial fibres (less than 4 mm depth within the muscle), aligned with the detection system (less than 5° misalignment), far from the end-plate and tendons. Values with more than 50% estimation error were obtained in the worst conditions (channels close to the innervation region or tendons, misalignment 10°, 6 mm depth of the fibre within the muscle).

Comparing the maximum likelihood and the reference point approaches, this study shows quite similar results obtained by such methods. In some of the simulated conditions, the reference point approach shows a lower sensitivity to the inhomogeneity of the volume conductor. Different methods for CV estimation have been compared in the literature, some papers stating the reference point method to be preferable [1][19], others indicating a lower estimation variance for the maximum likelihood approach [12][35]. As only single fibre action potentials for one anatomy (for example, a constant fat conductivity and thickness, a constant muscle fibre length) were simulated with no additive noise, the shown results provide only a representative example of application of the simulation model. Further simulation studies are needed to investigate the effect of the inhomogeneity of the considered volume conductor on sEMG signals and to assess the sensitivity of different algorithms for parameter extraction.

In conclusion, this study presents the modelling and derivation of the analytical solution of the problem of sEMG signals generation for the inhomogeneous, anisotropic, non space invariant triangular muscle tissue. The model may help in better understanding the generation of sEMG signals from complex muscle architectures and in interpreting experimental results. As an example of application, the problem of muscle fibre CV estimation was addressed.

APPENDIX
 Scale properties of the impulse response
Let's consider an impulse source placed at an arbitrary point. Without loss of generality, such a position of the impulse source can be expressed as $\vec{r}_s = (\rho = R, \theta = 0, z = 0)$, i.e. with vanishing angular and z variables, and R an arbitrary constant.

With the following change of variables

$$(r,\theta,Z) = \left(\frac{\rho}{R}, \theta, \frac{z}{R}\right) \quad , \quad \Phi = R\varphi \qquad (5)$$

we obtain that $\Phi(r,\theta,Z)$ solves Eq. (2) with R=1. Hence, the impulse response at a generic point can be expressed in terms of the solution for the problem with the impulse placed at R=1. The potential at the surface z=z$_0$ can be expressed as $\varphi(\rho,\theta,z_0) = \frac{1}{R}\Phi\left(\frac{\rho}{R},\theta,\frac{z_0}{R}\right)$. Let's consider the case R>1 (similar considerations hold for the case R<1). The potential Φ is detected at $z = \frac{z_0}{R}$, which is closer to the impulse than the surface z=z$_0$. In general, detecting at a surface which is closer to the source, the potential presents a larger amplitude and is less filtered by the volume conductor, which means that it has a larger frequency band. We can note that the division by R of the potential Φ reduces the amplitude and the change of variable $r = \frac{\rho}{R}$ scales the frequency content of the surface potential Φ.

The scaling properties of the volume conductor do not imply that the signal detected in time domain at different locations is only scaled during propagation (note for example that both ρ and z are scaled).

In this study, all impulse responses with impulses placed at sample points along a fibre path were simulated. An alternative simulation procedure exploits the scaling properties just explained. Indeed, sEMG simulation can be obtained by solving only one impulse response, saving computational time. A drawback of this method is that the sampling of both spatial frequencies and radial coordinate should be very careful, in order to avoid aliasing and low resolution in the worst case. Indeed, also the sample step is scaled when scaling properties are applied. A sampling frequency satisfying Nyquist theorem in all the configurations considered must be used in order to preserve information. Furthermore, the scaling of the radial variable requires interpolation when working in a discrete domain.

REFERENCES

[1] Arabadzhiev T.I., Dimitrov G.V., Dimitrova N.A., "Simulation analysis of the ability to estimate motor unit propagation velocity non-invasively by different two-channel methods and types of multi-electrodes", J. Electromyogr. Kinesiol., vol. 13, pp. 403-415, 2003.
[2] Blok J.H., Stegeman D.F., van Oosterom A., "Three-layer volume conductor model and software package for applications in surface electromyography", Ann. Biomed. Eng., vol. 30, pp. 566-577, 2002.
[3] Broman H., Bilotto G., De Luca C., "A note on non invasive estimation of muscle fiber conduction velocity", IEEE Trans. Biomed. Eng., vol. 32, pp. 341-343, 1985.

[4] Clark J., Plonsey R., "The extracellular potential field of the single active nerve fiber in a volume conductor", Biophys. Journ., vol. 8, pp. 842-64, 1968.
[5] Dimitrov G.V., Disselhorst-Klug C., Dimitrova N.A., Schulte E. and Rau G., "Simulation analysis of the ability of different types of multi-electrodes to increase selectivity of detection and to reduce cross-talk", J. Electromyogr. Kinesiol., vol. 13, pp. 125-38, 2003.
[6] Dimitrova N.A., Dimitrov G.V., "Interpretation of EMG changes with fatigue: facts, pitfalls, and fallacies", J. Electromyogr. Kinesiol., vol. 13, pp. 13-36, 2003.
[7] Disselhorst-Klug C., Silny J., Rau G., "Improvement of spatial resolution in surface-EMG: a theoretical and experimental comparison of different spatial filters", IEEE Trans. Biomed. Eng., vol. 44, pp. 567 – 574, 1997.
[8] Duchene J., Hogrel J.Y., "A model of EMG generation", IEEE Trans. Biomed. Eng., vol. 47, pp. 192-201, 2000.
[9] Farina D., Muhammad W., Fortunato E., Meste O., Merletti R., Rix H., "Estimation of single motor unit conduction velocity from surface electromyogram signals detected with linear electrode arrays", Med Biol Eng Comput., vol. 9, pp. 225-236, 2001.
[10] Farina D., Merletti R., "A novel approach for precise simulation of the EMG signal detected by surface electrodes", IEEE Trans. Biomed. Eng., vol. 48, pp. 637-646, 2001.
[11] Farina D., Merletti R.., "A novel approach for estimating muscle fiber conduction velocity by spatial and temporal filtering of surface EMG signals", IEEE Trans. Biomed. Eng., vol. 50, pp. 1340-1351, 2003.
[12] Farina D., Merletti R., "Methods for estimating muscle fiber conduction velocity from surface electromyographic signals", Med. Biol. Eng. Comput., vol. 42, pp. 432-445, 2004.
[13] Farina D., Mesin L., Martina S., Merletti R., "Comparison of spatial filter selectivity in surface myoelectric signal detection – Influence of the volume conductor model", Med. Biol. Eng. Comput., vol. 42, pp. 114-120, 2004.
[14] Farina D., Mesin L., Martina S., Merletti R., "A new surface EMG generation model with multi-layer cylindrical description of the volume conductor", IEEE Trans. Biomed. Eng., vol. 51, pp. 415-426, 2004.
[15] Farina D., Mesin L., Martina S., "Advances in surface EMG signal simulation with analytical and numerical descriptions of the volume conductor", Med. Biol. Eng. Comput., vol. 42, pp. 467-476, 2004.
[16] Farina D., Mesin L., "Sensitivity of surface EMG-based conduction velocity estimates to local tissue in-homogeneities – influence of the number of channels and inter-channel distance," J. Neurosci. Meth., vol. 142, pp. 83-89, 2005.
[17] Gootzen T.H., Stegeman D.F., Van Oosterom A., "Finite limb dimensions and finite muscle length in a model for the generation of electromyographic signals", Electroenc. Clin. Neurophysiol., vol. 81, pp. 152-162, 1991.
[18] Heringa A., Stegeman D.F., Uijen G.J., de Weerd J.P., "Solution methods of electrical field problems in physiology", IEEE Trans. Biomed. Eng., vol. 29, pp. 34-42, 1982.
[19] Hogrel J.Y., Duchene J., "Motor unit conduction velocity distribution estimation: assessment of two short-term

processing methods", Med. Biol. Eng. Comput., vol. 40, pp. 253-259, 2002.

[20] Kleine, B.U. Stegeman D.F., Mund D., Anders C., "Influence of motoneuron firing synchronization on SEMG characteristics in dependence of electrode position", J. Appl. Physiol., vol. 91, pp. 1588-1599, 2001.

[21] Lowery M.M., Stoykov N.S., Taflove A., Kuiken T.A., "A multiple-layer finite-element model of the surface EMG signal", IEEE Trans. Biomed. Eng., vol. 49, pp. 446-454, 2002.

[22] McGill K.C., Dorfman L.J., "High-resolution alignment of sampled waveforms", IEEE Trans. Biomed. Eng., vol. 31, pp. 462-468, 1984.

[23] Merletti, R., Lo Conte, L., Avignone, E. and Guglielminotti, P., "Modelling of surface myoelectric signals – part I: model implementation", IEEE Trans. Biomed. Eng., vol. 46, pp. 810-820, 1999.

[24] Merletti R., Roy S.H., Kupa E., Roatta S., Granata A., "Modeling of surface myoelectric signals--Part II: Model-based signal interpretation", IEEE Trans. Biomed. Eng., vol. 46, pp. 821-9, 1999.

[25] Mesin L., Farina D., "Simulation of surface EMG signals generated by muscle tissues with in-homogeneity due to fiber pinnation", IEEE Trans. Biomed. Eng., vol. 51, pp. 1521-1529, 2004.

[26] Mesin L., Farina D., "A model for surface EMG generation in volume conductors with spherical in-homogeneities", IEEE Trans. Biomed. Eng., vol. 52, pp. 1984 - 1993, 2005.

[27] Mesin L., Farina D., "An analytical model for surface EMG generation in volume conductors with smooth conductivity variations", IEEE Trans. Biomed. Eng., in press, 2006.

[28] Mesin L., Joubert M., Hanekom T., Merletti R., Farina D., "A Finite Element Model for Describing the Effect of Muscle Shortening on Surface EMG", IEEE Trans. Biomed. Eng., vol. 53, pp. 593 – 600, 2006.

[29] Mesin L., "Analytical Generation Model of Surface Electromyogram for Multi Layer Volume Conductors", in Modelling in Medicine and Biology VI, WIT Press, pp. 95-110, Proceedings Biomedicine 2005, Bologna 7-9 September 2005.

[30] Naeije M., Zorn H., "Estimation of the action potential conduction velocity in human skeletal muscle using the surface EMG cross-correlation technique" Electromyogr. Clin. Neurophysiol., vol. 23, pp. 73-80, 1983.

[31] Parker P.A., Scott R.N., "Statistics of the myoelectric signal from monopolar and bipolar electrodes", Med. Biol. Eng., vol. 11, pp. 591-596, 1973.

[32] Roeleveld K., Blok J.H., Stegeman D.F., van Oosterom A., "Volume conduction models for surface EMG; confrontation with measurements", J. Electromyograph. Kinesiol., vol. 7, pp. 221-232, 1997.

[33] Rosenfalck P., "Intra and extracellular fields of active nerve and muscle fibers. A physico-mathematical analysis of different models," Acta Physiol. Scand., vol. 321, pp. 1-49, 1969.

[34] Schneider J., Silny J., Rau, G., "Influence of tissue inhomogeneities on noninvasive muscle fiber conduction velocity measurements investigated by physical and numerical modeling", IEEE Trans. on Biomed. Eng., vol. 38, pp. 851-860, 1991.

[35] Schulte E., Farina D., Rau G., Merletti R., Disselhorst-Klug C., "Single motor unit analysis from spatially filtered surface electromyogram signals. Part 2: conduction velocity estimation", Med. Biol. Eng. Comput., vol. 41, pp. 338-345, 2003.

[36] Stegeman, D.F., Blok, J.H., Hermens, H.J. and Roeleveld, K., "Surface EMG models: properties and applications", J. Electromyograph. Kinesiol., vol. 10, pp. 313-326, 2000.

[37] van Oosterom A., "Principles in inverse electrophysiological modeling", 6th Deliverable of the SENIAM project, pp. 37-44, 1998.

Luca Mesin graduated in electronics engineering in December 1999 from Politecnico di Torino, Torino, Italy, he received the Ph.D. in Applied Mathematics in 2003, from the same university. Since March 2003, he is a Fellow of the Laboratory for Neuromuscular System Engineering in Torino. He was involved in research activities in the fields of Kinetic theory and Deformable Porous Media theory, with applications to Biomathematics and Composite Materials. Now, his main research interests concern signal processing of biomedical signals and modeling of biological systems.